Ha, J.H., and Gourlay, T.P. (2018). "Validation of Container Ship Squat Modeling Using Full-Scale Trials at the Port of Fremantle." *Journal of Waterway, Port, Coastal, and Ocean Engineering*, 144(1), DOI: 10.1061/(ASCE)WW.1943-5460.0000425.

Validation of Container Ship Squat Modeling Using Full-Scale Trials at the Port of Fremantle

Jeong Hun Ha[1] and Tim Gourlay[2]

[1] Ph.D. Candidate, Centre for Marine Science and Technology, Curtin University, Bentley, WA 6102, Australia (corresponding author). E-mail: jeonghun.ha@postgrad.curtin.edu.au

[2] Director, Perth Hydro Pty Ltd, Perth, WA 6000, Australia. www.perthhydro.com

Abstract

In this paper, selected results are presented from a set of recent full-scale trials measuring dynamic sinkage, trim and heel of sixteen container ship transits entering and leaving the Port of Fremantle, Western Australia. Measurements were made using high-accuracy GNSS (Global Navigation Satellite System) receivers and a fixed reference station. Measured dynamic sinkage, trim and heel of three example container ship transits are discussed in detail. Maximum dynamic sinkage and dynamic draught, as well as elevations of the ship's keel relative to Chart Datum, are calculated. A theoretical method using slender-body shallow-water theory is applied to calculate sinkage and trim for the transits. It is shown that the theory is able to predict ship squat (steady sinkage and trim) with reasonable accuracy for container ships at full-scale in open dredged channels. In future work, the measured ship motions, along with full measured wave time-series data, will be used for validating wave-induced motions software.

Author keywords: Squat; Ship UKC; Approach channel; Shallow water; Container ships.

Introduction

Since the 1990s, full-scale measurements on dynamic ship motions in waterways have been successfully carried out with the increasing accuracy of the Global Navigation Satellite System (GNSS) (Feng and O'Mahony 1999; Härting and Reinking 2002; Gourlay and Klaka 2007; Ha et al. 2016). These trials have played important roles in furnishing accurate and reliable full-scale data that may be utilized by ports, pilots and deck officers. Model-scale tests, being in a controlled environment, remain the method of choice for benchmarking studies (Mucha et al. 2014; Gourlay et al. 2015b), with appropriate allowance for scale effects (Graff et al. 1964; Deng et al. 2014).

Conducting full-scale trials involves a great deal of time and requires thorough preparation and close collaboration with pilots, port terminals, shipping agents and port VTS (Vessel Traffic Service). Care must be taken not to interfere with port operations, nor delay the normal pilotage. In addition, with regard to validation of numerical ship motion modelling at full-scale, there are uncertainties in applying theoretical methods to actual transit conditions, such as: seabed conditions; varying bathymetry; ever-changing waves, wind and currents; and commercial ships whose lines plans are confidential. Despite the difficulties in implementation and application, measurements and validations at full-scale provide an important practical test of numerical Under-Keel Clearance (UKC) modelling.

In April 2016, at the Port of Fremantle, Western Australia's largest general cargo port, the authors performed full-scale trials on 16 container ship transits, including 7 inbound and 9 outbound transits, via the Deep Water Channel, Entrance Channel and Inner Harbour (see chart AUS112 and 113). The purpose of the trials is not only to obtain high-quality data on vertical ship motions in the port approach channels including squat and wave-induced motions, but also to validate current UKC practice using the data from the measurements. Here, dynamic sinkage, trim and heel of three example container ships over their entire transits can be calculated by comparing the vertical motions when underway to the stationary condition at the berth. The dynamic draught and UKC at each point on the ship in the approach channels are also calculated. The net UKC and risk of running aground are then governed by the maximum dynamic draught over all of the most vulnerable hull extremities, i.e. the Forward Perpendicular (FP), Aft Perpendicular (AP), and port and starboard bilge corners (Gourlay 2007). Such data accumulation of the full-scale measurements will be of importance to comprehensive guidelines for minimum UKC.

Details of ship motion trials

Measurements were made on 16 container ship transits in total using the shore-based receiver method, which uses high-accuracy GNSS receivers onboard as well as a fixed base station for an external reference. Raw data from the trials has been published as a CMST (Centre for Marine Science and Technology) report (Ha and Gourlay 2016). The general process of full-scale trials and the shore-based receiver method are described in Gourlay and Klaka (2007) and Ha et al. (2016). Data recording covers a period of time before departure or after arrival to take a stationary

reading at the berth. In the present trials, data recording was commenced prior to leaving the berth for the outbound transits and continued until after all mooring work had been completed for the inbound transits. The at-berth measurements were then used as a reference value for comparing the vertical height measurements while underway.

Description of the ships and transit conditions

The following criteria have been taken into account in choosing example transits for further analysis:

- A transit should have no suspicious data or ambiguity problems in any measurement results, and hence should be considered as a set of high-quality data
- Hydrostatic data at an actual transit draught should have been obtained during trials to assist with ship motion validation. This data is obtained from the ship's Trim and Stability Book
- For validating ship motion predictions, there should be a published representative ship model that has similar characteristics to the actual ship. Ships should be fairly modern, so that analysis can keep pace with contemporary trends in ship design
- Relevant environmental data such as waves, wind and tides should be obtained

On this basis, three transits have been chosen for analysis: *SEAMAX STAMFORD*, built in 2015, a Post-Panamax container ship with a capacity of 4,896 TEU; *MOL PARAMOUNT*, built in 2005, a Post-Panamax container ship with a capacity of 6,350 TEU; and *CMA CGM WAGNER*, built in 2004, a Post-Panamax container ship with a capacity of 5,782 TEU. Details of these ships are shown in Table 1. Displacement and block coefficient (C_B) are values at summer draught. Block coefficient (C_B) is the ratio of displaced volume to (L_{PP}.Beam.Draught). MOL PARAMOUNT and CMA CGM WAGNER have similar ship dimensions, and they have slightly lower C_B than SEAMAX STAMFORD.

Table 1. Details of the container ships

Particulars	SEAMAX STAMFORD	MOL PARAMOUNT	CMA CGM WAGNER
L_{OA} (m)	250.00	293.19	277.28
L_{PP} (m)	238.35	276.00	263.00
Beam (m)	37.30	40.00	40.00
Depth (m)	19.60	24.30	24.30
Summer Draught (m)	13.00	14.02	14.52
Displacement (ton)	79,702.00	99,620.00	96,997.00
C_B (-)	0.673	0.628	0.620

During the transits, the authors were able to view the ship's Trim and Stability Book and take photos of relevant operation conditions. Comparative transit conditions for all the ships are shown in Table 2. Note that C_B is calculated based on arrival draught. Longitudinal centre of buoyancy (LCB) and longitudinal centre of floatation (LCF) are given as metres forward of the AP. Average draught is represented for C_B, LCB and LCF. GM_f is metacentric height, corrected for free surface effect. As shown in Table 2, MOL PARAMOUNT has a level static trim, whereas SEAMAX STAMFORD and CMA CGM WAGNER statically trim stern-down at their arrival by 0.85m and 1.50m respectively.

Table 2. Details of the transit conditions

Particulars	SEAMAX STAMFORD	MOL PARAMOUNT	CMA CGM WAGNER
Date and Time	17/04/2016 04:27AM ~ 05:47AM	21/04/2016 03:11AM ~ 04:32AM	25/04/2016 04:12AM ~ 05:31AM
Direction	Inbound	Inbound	Inbound
Draught fwd (m)	10.40	11.39	10.00
Draught aft (m)	11.25	11.39	11.50
Arrival displacement (ton)	62,584.00	73,926.90	63,569.00
C_B (-)	0.634@10.83	0.574@11.39	0.548@10.75
LCB (m)	117.79@10.85	133.06@11.40	-
LCF (m)	111.68@10.85	126.05@11.40	-
GM_f (m)	3.88	3.87	4.51

Ship motions were measured using JAVAD GNSS® Triumph-1™ and Triumph-2 ™ receivers. Four receivers were used for each set of measurements, with one in each of the following locations:

- Base station fixed to pilot jetty
- Roving receiver fixed to ship bow
- Roving receiver fixed to port bridge wing
- Roving receiver fixed to starboard bridge wing

A typical GNSS equipment setup at the Port of Fremantle is shown in Fig. 1. With reference to Fig. 1(b), the base station was placed at the same point (32° 2.52236' S, 115° 45.19799' E) on the pilot jetty for all transits, as shown in Fig. 2.

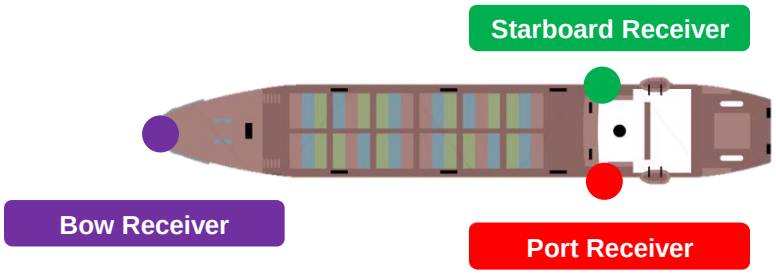

(a)

(b) (c) (d) (e)

Fig. 1. GNSS receivers setup: (a) Plan view of ship receivers; (b) Base station on pilot jetty in the CMA CGM WAGNER transit; (c) Bow receiver in the MOL PARAMOUNT transit; (d) Port receiver on bridge wing in the SEAMAX STAMFORD transit; (e) Starboard receiver on bridge wing in the SEA MAX STAMFORD transit (images by Jeong Hun Ha)

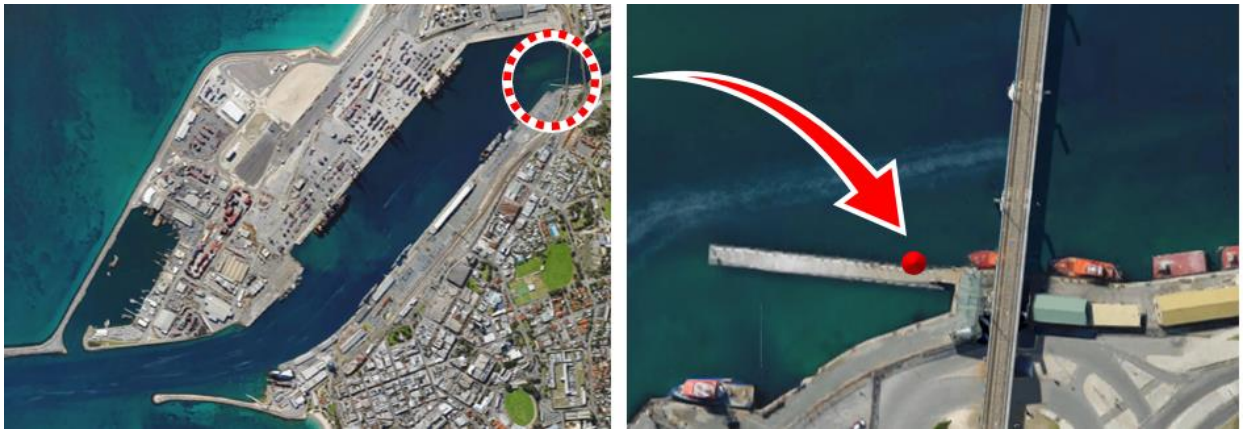

Fig. 2. Base station location on pilot jetty (Imagery ©2016 Google, Data SIO, NOAA, U.S. Navy, NGA, GEBCO, Map data © 2016 Google)

Description of the port, channels and measured ship tracks

Layout of the Port of Fremantle, its approach channels and buoys, together with tracks of the three inbound ships are illustrated in Fig. 3.

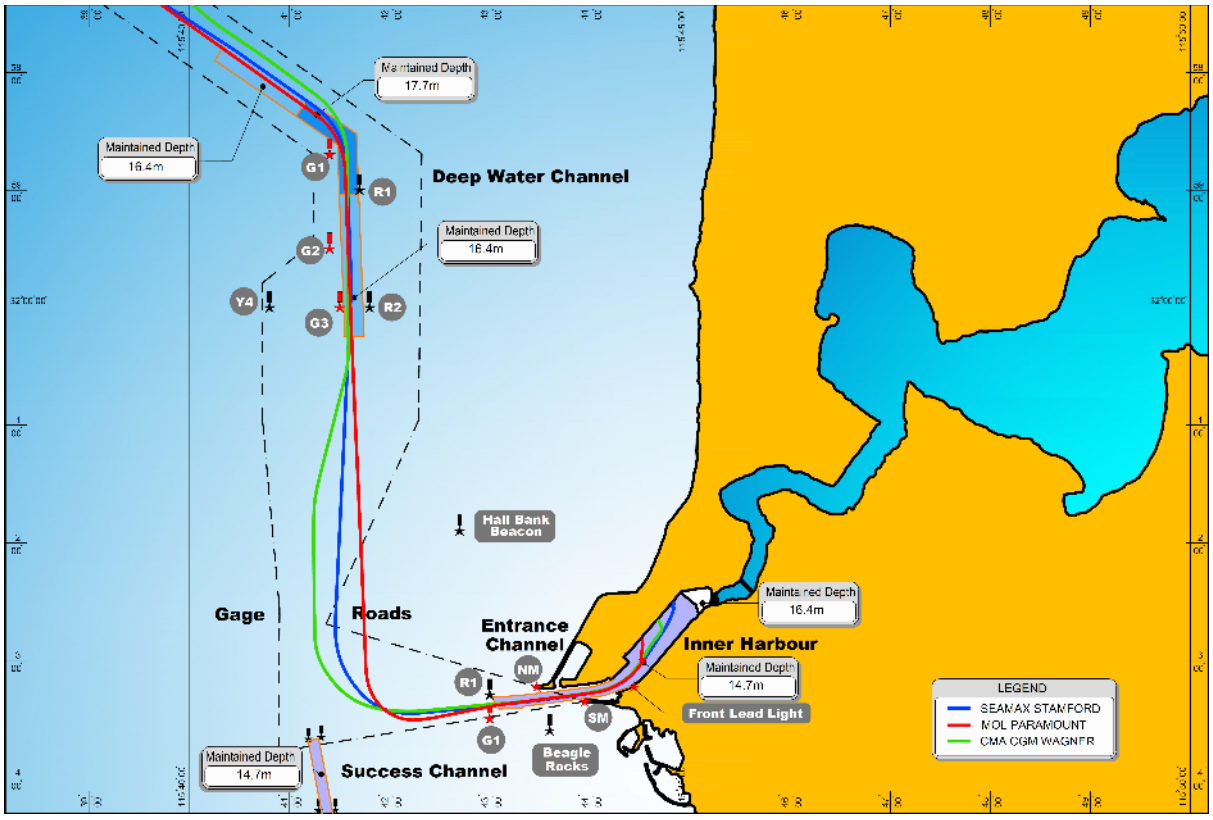

Fig. 3. Port of Fremantle approach channels and measured midship tracks

The port is operated with a marine section largely divided into three parts: the Deep Water Channel, around 3 nautical miles in length and 300m in width; the Entrance Channel, around 1 nautical mile from Front Lead Light to Green No.1 Buoy (G1) and width of 170m; and the Inner Harbour with a water area of approximately 82ha. The channels are varying in depth from 14.7m to 17.7m based on the Chart Datum, which is 0.756m below the Australian Height Datum (AHD, national vertical datum for Australia) and approximately the level of LAT (Lowest Astronomical Tide). An additional depth of up to 1.3m can be considered by tides, i.e. HAT (Highest Astronomical Tide) and MSL (Mean Sea Level) in the Port of Fremantle are 1.3m and 0.7m respectively (see chart AUS112). Details of tides can be found in the Australian National Tide Tables (ANTT, otherwise known as AHP11).

For the inbound ships, measurements were made from the moment all onboard receivers are set up, which is invariably before the ships move into the Deep Water Channel, until all mooring work is completed at the berth. All tracks look almost analogous to each other within the Deep Water Channel, but they have different paths to enter the Entrance Channel and hence different turning radius before the Entrance Channel. Different pilotage sequences may have been required, depending on diverse loading conditions as well as changing environmental conditions. With the fact that each pilotage was conducted by different pilots, different techniques could have also been applied.

Environmental data

Some of the wave data, measured at 1.28Hz by the Cottesloe wave buoy (31° 58.74333' S, 115° 41.39833' E) near Green No.1 Buoy (G1) in the Deep Water Channel, have been provided from collaboration with the Coastal infrastructure team from Western Australian Department of Transport (WA DoT). The full measured wave time-series data will be used to study wave-induced motions in the channel, in future work. This information is held in the onboard memory, and hence the data will be provided when WA DoT recovers the wave buoy for the next annual maintenance service. The wave data provided by WA DoT is presented in Fig. 4, where H_S is the significant wave height, T_S is the significant wave period, and T_P is the spectral peak period. Sea/swell cutoff is 8 seconds.

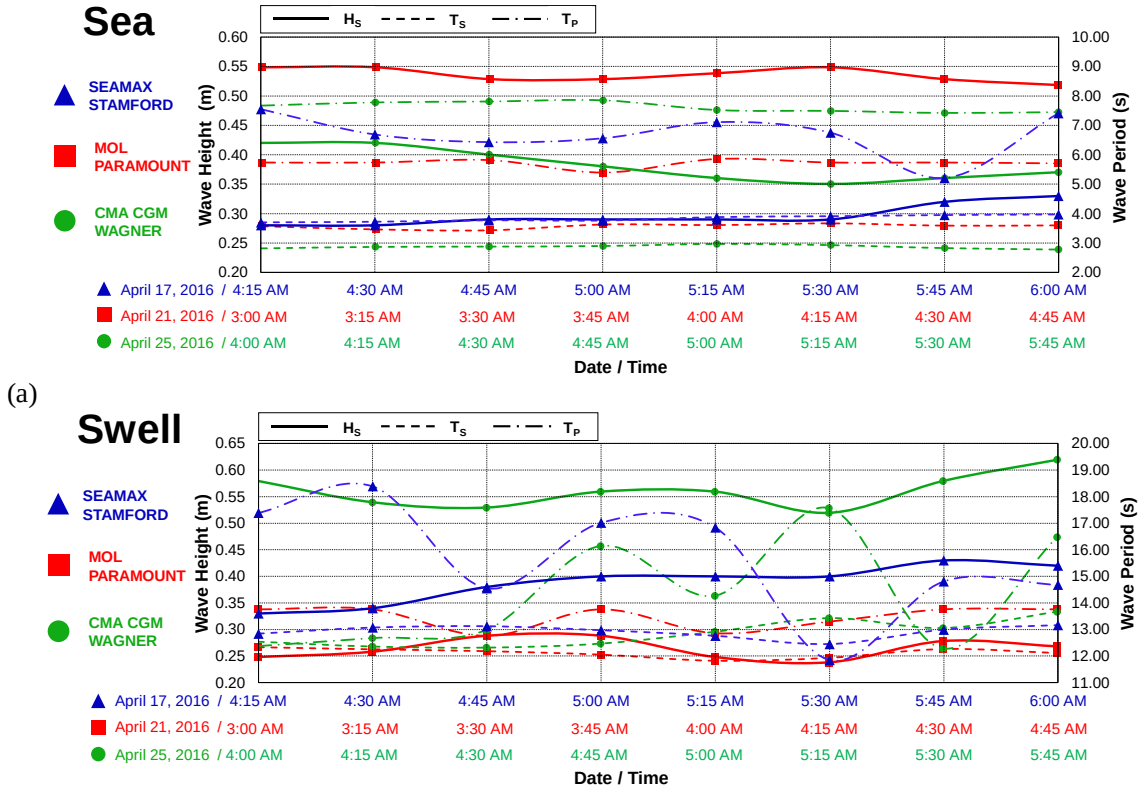

Fig. 4. Measured wave data during the transits: (a) sea; (b) swell

Regarding wind conditions, visual observations on wind speeds and directions were made and recorded by the authors during each ship transit, shown in Table 3. The full measured wind data can be obtained from the Australian Government Bureau of Meteorology (BoM) if required.

Table 3. Details of the observed wind conditions

Particulars	SEAMAX STAMFORD	MOL PARAMOUNT	CMA CGM WAGNER
Wind Speed	Calm	10 knots	10 - 15 knots
Wind Direction	Calm	Easterly	North-westerly

Measured tide in the Inner Harbour (32° 3.258' S, 115° 44.3718' E) in the Port of Fremantle has been provided by Fremantle Ports and then applied to calculate dynamic sinkage of the ships. The tidal datum is the same as the Chart Datum used in chart AUS112 and 113, and hence LAT (Lowest Astronomical Tide) at the Port of Fremantle. The tidal data covering the period of the present measurements is shown in Fig. 5.

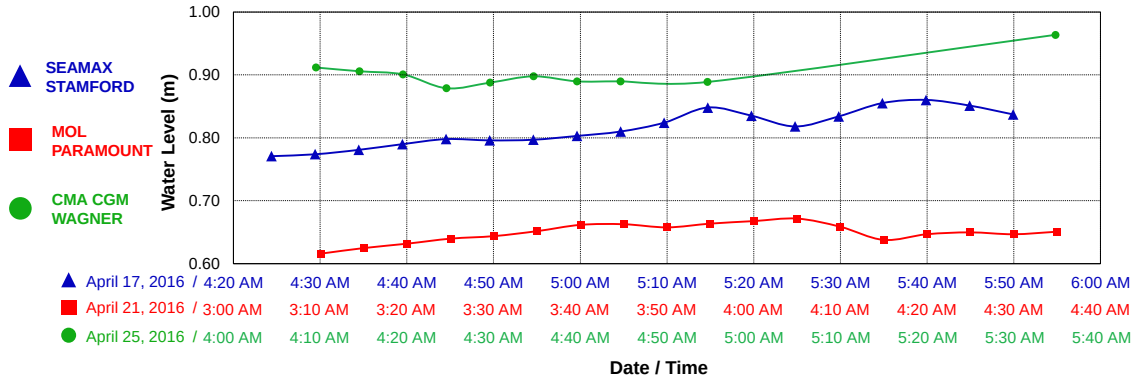

Fig. 5. Measured tidal data during the transits

The currents are usually quite weak. In Gage Roads (see Fig. 3), the currents move southward and northward, across the Entrance Channel, for approximately 14 and 10 hours respectively, which may generally attain a rate of 1 knot; however, during the winter months (June-August), these currents may attain rates up to 2 knots (NGA 2014; U.S. NRL n.d.). Note that no current measurement has been made for the present trials.

Water density can vary from the area of the Entrance Channel and Inner Harbour to the Deep Water Channel due to the port's geographic location in an estuary (Swan River Estuary). However, water density in the Inner Harbour is stated to be 1.025 g/cm^3, generally at all tides (Fremantle Ports 2011), which means there may be a delicate difference in water density between inside and outside of the port most of time. A heavy rainfall can cause a variation in water density in the Inner Harbour and Entrance Channel, but such a situation did not arise during the present measurements.

Bathymetric data

To give the keel heights relative to the seabed, detailed survey data for the Deep Water Channel, Entrance Channel and Inner Harbour, as provided by Fremantle Ports, have been used. The data is originally from Fremantle Ports' annual Hydrographic Survey, carried out in September and October 2015, and composed of 144,150 survey points for the Entrance Channel and Inner Harbour, and 90,566 survey points for the Deep Water Channel. Fig. 6 shows the survey points in the channels together with an example ship track (SEAMAX STAMFORD, inbound).

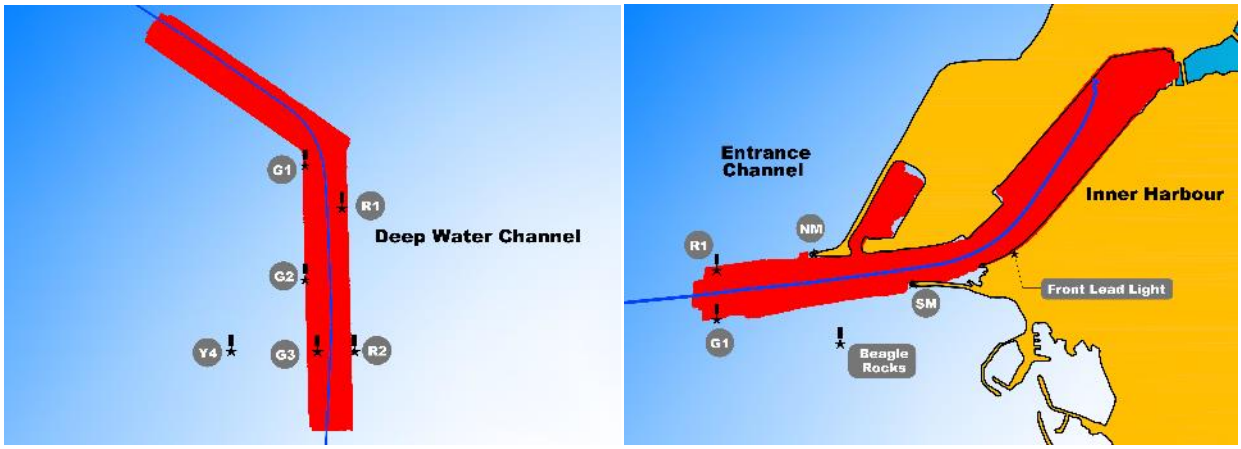

(a) (b)

Fig. 6. Bathymetric data from Fremantle Ports' annual Hydrographic Survey: (a) the Deep Water Channel; (b) the Entrance Channel and Inner Harbour

In order to more accurately compare the ship's keel heights and the seabed, water depths along the track should be taken from the bathymetric data. Z-values of the survey points that are the closest points to the track on the plane have been extracted, using MATLAB®, Microsoft® Excel software and AutoCAD® software. A comparison between the bathymetry based on AUS112 and that extracted is shown in Fig. 7. A flat and dashed seabed line is based on the charted depth on AUS112, and a fluctuating seabed line is the actual survey line provided by Fremantle Ports.

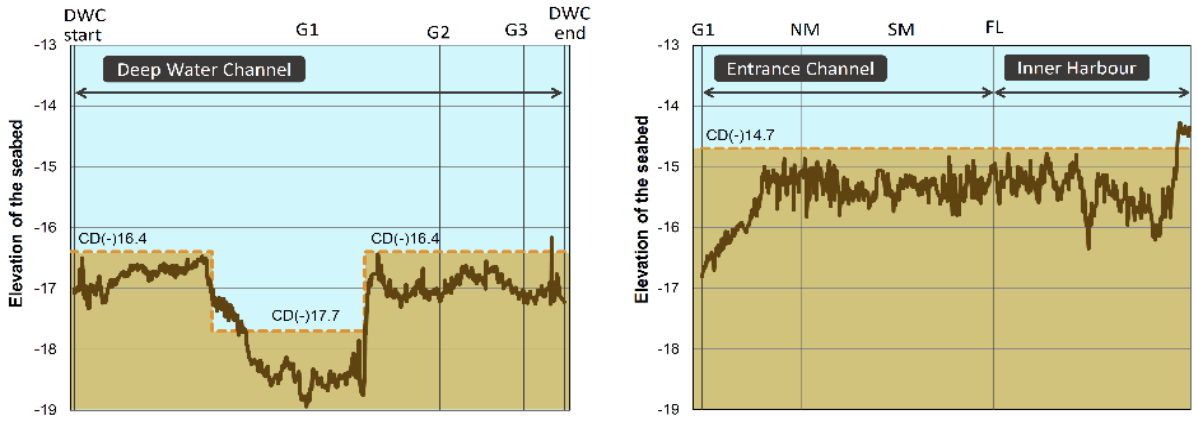

(a) (b)

Fig. 7. Comparison of the seabed lines based on the chart and the survey: (a) the Deep Water Channel; (b) the Entrance Channel and Inner Harbour

Measured dynamic sinkage, trim and heel

All data was recorded at 1.0 Hz and post-processed using the Trimble® Business Centre software. The raw GNSS results for each receiver have been combined to give the sinkage at the forward,

aft and transverse extremities of the keel that would be a point of concern of running aground. Dynamic trim and heel can then be calculated by assuming the ship to be rigid and comparing trim and heel angles relative to the static floating position (Gourlay 2008a). No additional hogging or sagging of the ship while underway is considered. A method and important height components for calculating sinkage from the raw GNSS height measurements are described in Gourlay and Klaka (2007) and Ha et al. (2016).

Error analysis

Vertical position accuracy of the JAVAD GNSS® Triumph-1™ and Triumph-2 ™ receivers is specified to be within 15mm + 1ppm*(baseline length) in JAVAD GNSS® (2012) and JAVAD GNSS® (2015). Expected vertical RMS (root-mean-square) errors for the transits were captured in the baseline processing of the Trimble® Business Centre software. These were in the range of 0.011m and 0.012m, and the RMS error in the GNSS receiver's vertical position is estimated to be less than 0.012m.

GNSS heights are referenced to an ellipsoid, and geoid undulation (N) is required to convert ellipsoidal heights to orthometric heights. GDA94 (the Geocentric Datum of Australia) and AUSGeoid09, which is the Australia-wide gravimetric quasigeoid model, have been applied to transfer between the raw GNSS heights and the Australian Height Datum (AHD) heights. According to Featherstone et al. (2011) and Brown et al. (2011), the RMS error of ± 0.030m was found in using the AUSGeoid09.

The stationary reading at the berth was taken based on 3 minute-averaged values of the ship's vertical motion since the end of the mooring works. However, the static floating position of the ships still had some residual vertical movement due to seiches in the Inner Harbour. The RMS error from each receiver on the ships, for the last three minutes after completion of mooring operations, ranged from 0.009m to 0.016m. The RMS error in the static reading is, therefore, estimated to be less than 0.016m.

Equipment error in the tide gauge should also be considered as an error component in calculating dynamic sinkage. The expected RMS error in tide gauges themselves would be typically 0.010m (Verstraete 2001; Gourlay and Klaka 2007).

As mentioned previously, the local tide data recorded at 5-minute intervals has been provided by Fremantle Ports. In order to apply this data to dynamic sinkage of the ships measured at 1-second intervals, a linear interpolation method was used to find tidal elevation at a particular point, i.e. at 1.0 Hz. The RMS error in the interpolation method ranged between 0.006m and 0.010m for the three ships, and hence estimated to be less than 0.010m.

In addition, the tidal data from the tide gauge in the Inner Harbour (32° 3.258' S, 115° 44.372' E) of the Port of Fremantle has been used for the entire transit including the section of the Deep Water Channel, even though the end of the Deep Water Channel is approximately 6.5 nautical miles away from the gauge. By comparing measured tidal data from other stations nearby the Port of Fremantle, an error in tidal elevation due to sea surface slope can be estimated (Gourlay and Klaka 2007). Hourly tidal observations in Hillarys Boat Harbour (31° 49.536' S, 115° 44.316' E), located around 13.5 nautical miles away from the Port of Fremantle, have been provided by the National Tidal Unit (NTU) from the Australian Government Bureau of Meteorology (BoM). As the tidal data from each tide gauge has been referenced to different vertical datums, a temporary datum should be made for putting these time series of tide observations together. It is assumed that the level of local MSL based on each datum will be the same. The difference in tidal elevation between the two stations can then be found using the level of the local MSL as a common datum.

As shown in Fig. 8, tidal elevation relative to the local MSL for the Port of Fremantle and Hillarys Boat Harbour has been compared to estimate the error. As a result, for the three days when the ship trials were carried out, the RMS error of the observed tidal data from the two stations ranged from 0.013 to 0.021m. Assuming the Deep Water Channel lies halfway between the Port of Fremantle and Hillarys Boar Harbour, the RMS error in the discrepancy of tidal elevation application is zero near the Inner Harbour and Entrance Channel, and less than 0.010m in the Deep Water Channel.

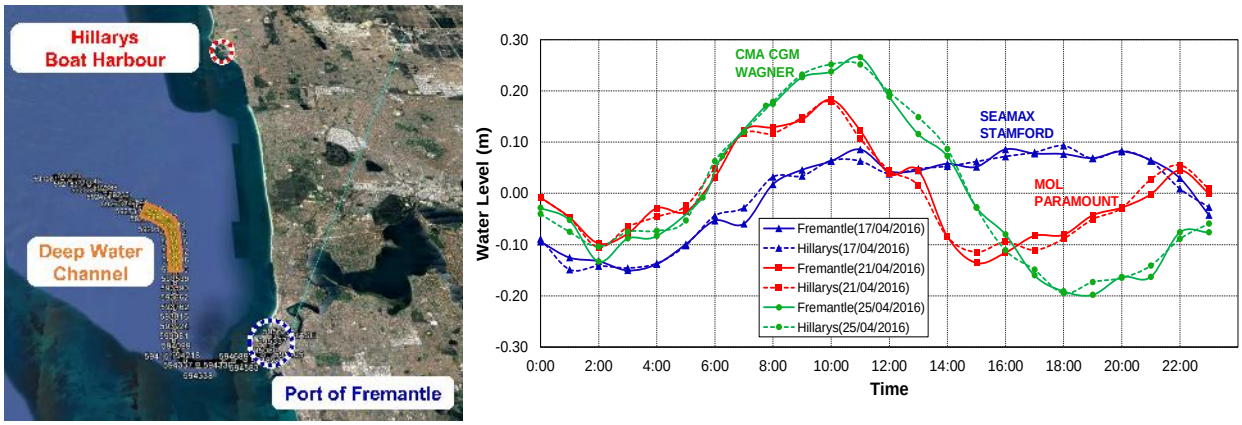

(a) (b)

Fig. 8. (a) Geographical location of the Port of Fremantle, Hillarys Boat Harbour and Deep Water Channel (©2016 Google, Image ©2016 DigitalGlobe, Data SIO, NOAA, U.S. Navy, NGA, GEBCO); (b) tidal elevation relative to local MSL for the Port of Fremantle and Hillarys Boat Harbour

The RMS errors inherent in calculating dynamic sinkage of the ship transits in the channels are summarized in Table 4. For the final dynamic sinkage results, all height components, including the above-mentioned sources, are added or subtracted (Gourlay and Klaka 2007; Ha et al. 2016), and hence the total RMS error is the square root of the sum of the squares of the error for each factor (Gourlay 2008b), i.e. 40mm in the Deep Water Channel, and 39mm in the Entrance Channel and Inner Harbour.

Table 4. Estimated RMS errors in calculating dynamic sinkage

Error factors	Deep Water Channel	Entrance Channel & Inner Harbour
Error in the GNSS receivers	0.012 m	0.012 m
Error in Geoid undulation N (AUSGeoid09)	0.030 m	0.030 m
Error in the static reading at the berth	0.016 m	0.016 m
Error in the tide gauge (equipment failure)	0.010 m	0.010 m
Error in interpolating to find tidal elevation at a particular point (at 1.0 Hz)	0.010 m	0.010 m
Error in the discrepancy of tidal elevation due to sea surface slope	0.010 m	-
Total	0.040 m	0.039 m

If a large number of the trials were carried out in the same conditions, the total RMS error would be the standard deviation of the measured dynamic sinkage (Gourlay 2008b). The errors depend on assuming a distribution to be normal (or Gaussian), and so about 95% of the actual dynamic sinkage usually fall within 2 standard deviations of the mean. Therefore, with a 95% confidence,

the actual dynamic sinkage will lie within the margin of error of ± 0.080m in the Deep Water Channel, and ± 0.078m in the Entrance Channel and Inner Harbour.

Dynamic sinkage

As shown in Fig. 9, vulnerable extremities of container ships differ from those of bulk carriers, which have relatively longer parallel midbodies. Positions of the port and starboard bilge corners of the container ships should, therefore, be defined properly as the widest points of the ship's keel where maximum sinkage could occur. The widest points are captured to be a little aft of amidships, approximately 47% of L_{PP} forward of the AP (see Fig. 9(a)), from the Deck and Profile drawing for SEAMAX STAMFORD. This proportion is also applied to MOL PARAMOUNT and CMA CGM WAGNER.

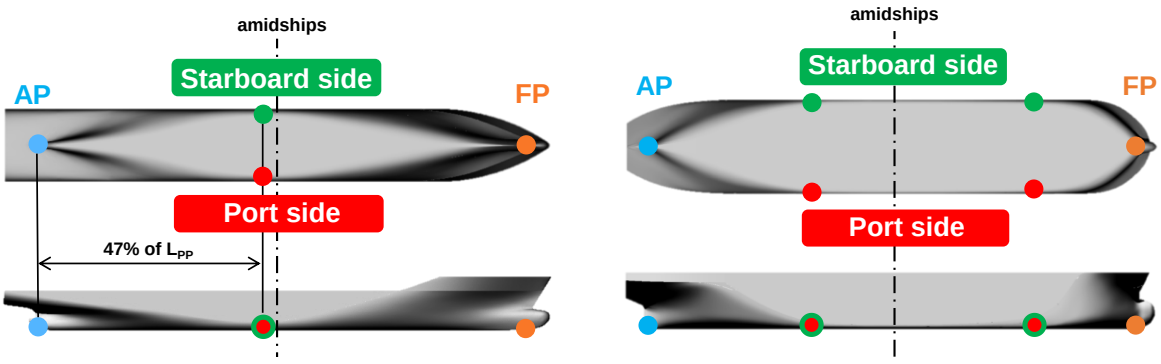

(a) (b)

Fig. 9. Hull extremities: (a) container ships; (b) bulk carriers

As for the transverse positions of the bilge corners, a distance of 78% of the half-beam away from the centreline of the ship has been taken from the body plans of the KCS (Lee et al. 2003) and FHR Ship D (Vantorre and Journée 2003; Gourlay et al. 2015b) hulls, and 82% for the DTC hull (el Moctar et al. 2012). All these hulls are considered to be representatives of container ship hulls which will be explained subsequently. Moreover, a distance of 82% of the half-beam away from the centreline of the ship has also been taken from the section of the General Arrangement Plan for CMA CGM WAGNER. The transverse positions of the bilge corners are taken as being at 80% of the half-beam away from the ship centreline in all cases.

Here, dynamic sinkage means the total sinkage, relative to the static floating position, that includes: a near-steady component due to the Bernoulli effect known as squat; an unsteady component due to wave-induced heave, pitch and roll; and a slowly-varying heel due to wind and turning. Measured sinkage, together with ship speed and channel bathymetry, are shown in Fig. 10. Results are plotted against cumulative distance from the Front Lead Light (FL) (32° 3.22728' S, 115° 44.45048' E). Vertical lines are shown for South Mole (SM), North Mole (NM) and Green No.1 Buoy (G1) in the Entrance Channel. In the Deep Water Channel (DWC), vertical lines are shown at the starting point, Green No.1 Buoy (G1), Green No.2 Buoy (G2), Green No.3 Buoy (G3) and the end point (see Fig. 3 and Fig. 6). Sinkage is given at the FP, AP, and port and starboard bilge corners (refer to Fig. 9(a)) and defined as being positive downward.

Fig. 10 clearly shows the effect of ship speed on sinkage. However, in the present trials, the speed of the three ships and the water depth decreased simultaneously in the deepest part of the Deep Water Channel, around the G1 buoy, thereby another important correlation between the sinkage and water depth is not independently captured. The ships all may have required decreasing their speed for turning manoeuvres in this curved section of the channel. Water depth in the unmaintained section (between the Deep Water Channel and Entrance Channel) is uncertain, and no detailed bathymetric survey data currently exists. According to charts AUS 112 and 113, water depth in that section is seen to be quite erratic with the depth range of about 15m and 20m, and, therefore, any interpretation on the correlation between the sinkage and water depth in the section is not made.

Maximum sinkage is observed at the starboard bilge corner in the area between the G2 and G3 buoy of the Deep Water Channel for MOL PARAMOUNT and CMA CGM WAGNER. Maximum sinkage occurs at the bow near the starting point of the Deep Water Channel for SEAMAX STAMFORD. SEAMAX STAMFORD has also large sinkage and oscillations, close to its maximum value, in between the G2 and G3 buoy. It may result from combined effect of residual heel oscillations due to rudder application and rate of turn (Gourlay 2008a), and dynamic trim due to acceleration (Ferguson and McGregor 1986; Hatch 1999), because a change in rudder application as well as an acceleration in ship speed were made in this part of the channel at the end of the turn (see Fig. 3).

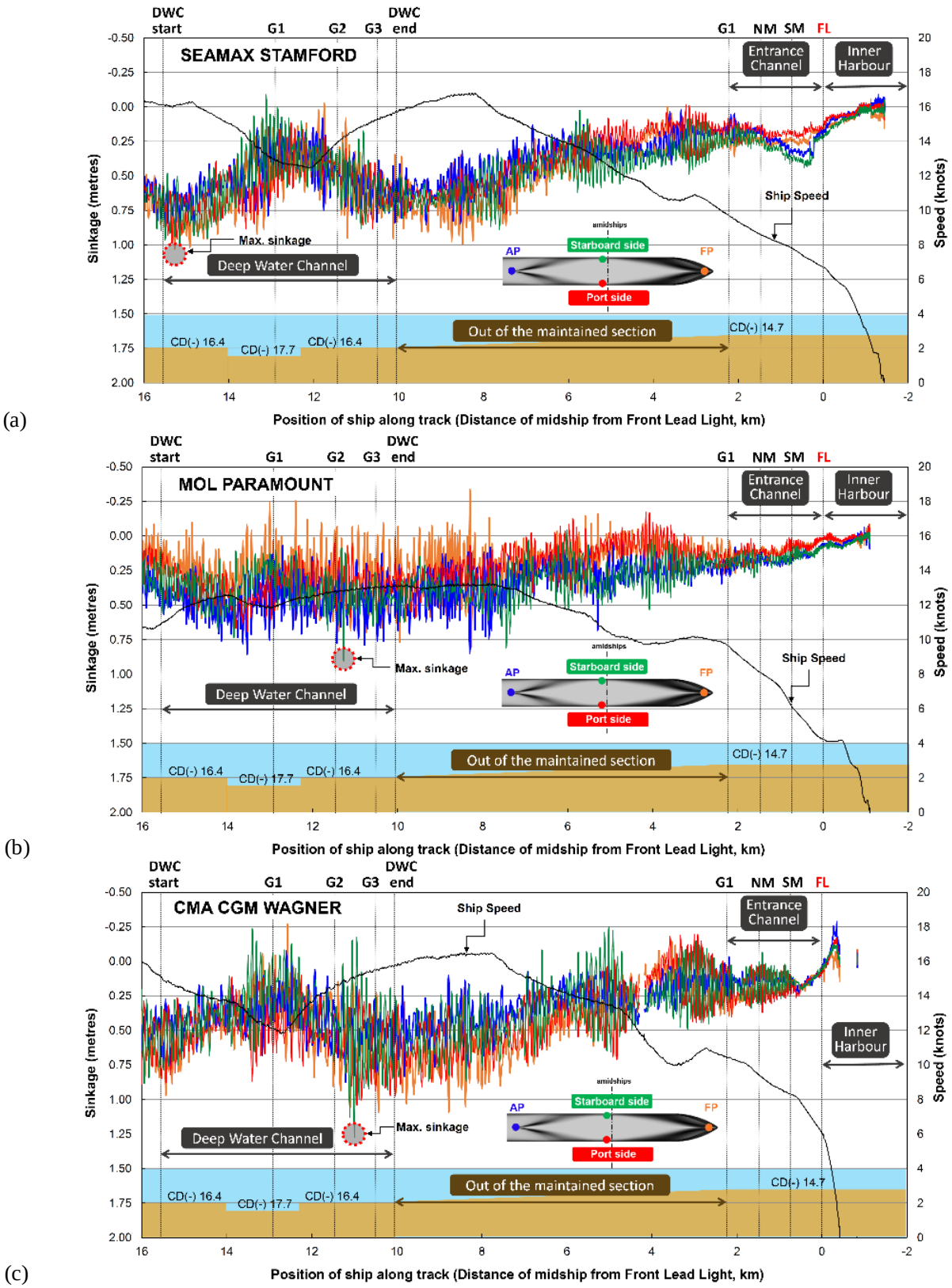

Fig. 10. Measured sinkage (positive downward) at four points: (a) SEAMAX STAMFORD; (b) MOL PARAMOUNT; (c) CMA CGM WAGNER (Note: Chart datum depth (not to scale) also shown)

The SEAMAX STAMFORD and CMA CGM WAGNER transits have similar ship speeds during their pilotage, and hence a similar trend in their vertical motions. Since the CMA CGM WAGNER transit was operated in relatively larger and longer period swell conditions (see Fig. 4), highly oscillatory vertical motions due to its wave-induced motions are seen in the result.

Maximum sinkage results for the ship transits are summarized in Table 5. SEAMAX STAMFORD has maximum sinkage at the bow, and the other two at the starboard bilge corner. However, for a ship with static stern-down trim, e.g. SEAMAX STAMFORD and CMA CGM WAGNER (see Table 2), the FP or starboard bilge corner having maximum sinkage may not be the closest point to the seabed. The stern can still have maximum dynamic draught due to its already close proximity to the seabed. Here, the dynamic draught at each location on the ship can be found by adding the static draught at that point to the sinkage at that point. The point on the ship with the maximum dynamic draught is the point most likely to hit the bottom, i.e. the AP for SEAMAX STAMFORD and CMA CGM WAGNER; the starboard bilge corner for MOL PARAMOUNT, as shown in Table 5.

Table 5. Measured maximum sinkage and dynamic draught, and dynamic draught increase for the ship transits

Ships	Maximum sinkage				Maximum dynamic draught		Dynamic draught increase	
	metres	point	% of L_{PP}	% of static draught	metres	point	metres	% of static draught
SEAMAX STAMFORD	1.03	FP	0.43	9.91	12.14	AP	0.89	7.87
MOL PARAMOUNT	0.91	Stbd Bilge	0.33	7.96	12.30	Stbd Bilge	0.91	7.96
CMA CGM WAGNER	1.27	Stbd Bilge	0.48	11.81	12.38	AP	0.88	7.62

Dynamic draught increase is, here, defined as the difference between the maximum dynamic draught and its static draught (Gourlay and Klaka 2007). This leads directly to decrease in Under-Keel Clearance (UKC), and hence is the most important consideration in avoiding grounding. Maximum sinkage and dynamic draught increase are also expressed as a percentage of the static draught of the ships to compare the results to conventional information on ship UKC or navigation.

For practical UKC management, the ship's vertical position should be plotted, relative to Chart Datum, so that the port may know the actual real-time clearance from the seabed. The appendix shows these vertical elevation changes. In addition, Table 6 shows an example calculation of sinkage and real-time UKC for SEAMAX STAMFORD at time of maximum measured sinkage, and so its FP (see Table 5) in the section with the water depth of 16.4 m in the Deep Water Channel (see Fig. 10). In comparison with Table 5, it is confirmed that maximum sinkage does not give maximum dynamic draught, since the AP has larger static draught. As the sinkage at the AP, for comparative purposes in Table 6, has been calculated from the raw GNSS results of each receiver, some elevations cannot be shown.

Table 6. Example calculation of sinkage and real-time UKC for SEAMAX STAMFORD

Calculations	Components		FP	AP	Note
Sinkage calculation	A	Static draught	10.40m	11.25m	
	B	Tide elevation at berth	(+) 0.85m CD	(+) 0.85m CD	
	C	Keel elevation at berth	(-) 9.55m CD	(-)10.40m CD	B-A
	D	Bow GNSS receiver elevation at berth	(+) 17.71m CD	-	
	E	Bow GNSS receiver elevation underway	(+) 16.61m CD	-	
	F	Bow sinkage relative to Chart Datum	1.10m	-	D-E
	G	Tide elevation underway	(+) 0.78m CD	(+) 0.78m CD	
	H	Sinkage relative to free surface water level	1.03m	0.88m	F+G-B
Real-time UKC calculation	I	Dynamic draught	11.43m	12.13m	A+H
	J	Water depth underway	(-) 16.40m CD	(-) 16.40m CD	
	K	Real-time UKC	5.75m	5.05m	(G-I)-J

The minimum real-time clearance in each section of varying water depth can then be captured by the calculation above. Calculated minimum real-time clearance in the Deep Water Channel, Entrance Channel and Inner Harbour, as well as the keel point where that occurs, are shown in Table 7 (see also Appendix). Tide ranges while underway in each channel are also shown so that tidal contributions to the minimum UKC can be roughly identified.

Table 7. Calculated minimum UKC for the ship transits

Ships	Deep Water Channel (charted depth: 16.4 - 17.7m)				Entrance Channel & Inner Harbour (charted depth: 14.7m)			
	metres	point	% of static draught	tide ranges	metres	point	% of static draught	tide ranges
SEAMAX STAMFORD	5.05	AP	44.90	0.78 - 0.80	3.93	AP	34.97	0.82 - 0.86
MOL PARAMOUNT	4.75	Stbd Bilge	41.68	0.63 - 0.65	3.67	Stbd Bilge	32.26	0.64 - 0.67
CMA CGM WAGNER	4.92	AP	42.76	0.88 - 0.90	3.82	AP	33.20	0.89 - 0.96

For the ships trimmed by the stern at arrival time, i.e. SEAMAX STAMFORD and CMA CGM WAGNER, the AP is the closest point to the seabed in both channels, but MOL PARAMOUNT with level static trim (see Table 2) has its minimum UKC at the starboard bilge corner. Note that the points closest to the seabed can be different in Table 5 and Table 7 because the maximum sinkage and dynamic draught for each ship have been captured through its whole transit, including sections out of the channels, whereas the minimum UKC for each ship has been calculated within the channels.

Dynamic trim

Dynamic trim is, here, the ship's total change in trim (positive stern-down), relative to the static floating position, that includes wave-induced pitch (Gourlay 2008a). So that trim is not swamped by wave-induced pitch, a low-pass filter with a cutoff period of 5 minutes has been applied to the dynamic trim results.

Measured dynamic trim for the three example transits is shown in Fig. 11. Note that dynamic trim is given in metres based on the difference between the FP and AP, and the filtered results are presented as the same colour as the measured, but thicker lines for each transit.

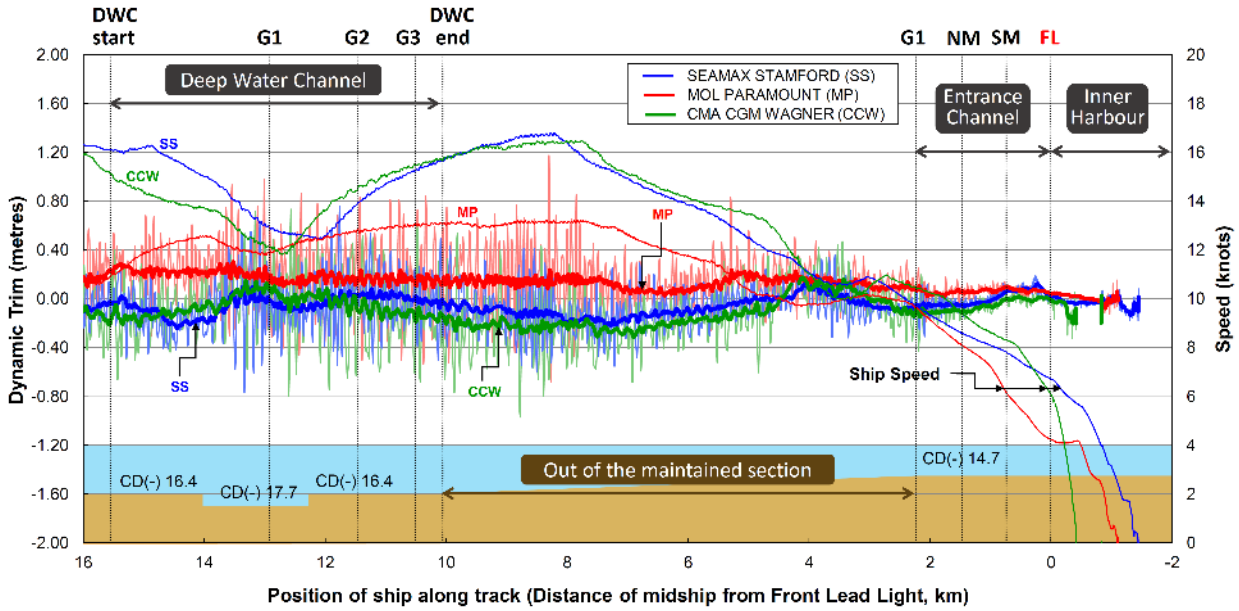

Fig. 11. Measured dynamic trim (positive stern-down) for the three ship transits (Note: Chart datum depth (not to scale) also shown)

Model-scale tests (Dand and Ferguson 1973; Gourlay 2006; Gourlay et al. 2016) and full-scale tests (Gourlay 2008b; Härting et al. 2009; Ha et al. 2016) show that bulk carriers have a tendency to trim by the bow when underway. No such tendency in trim is seen for container ships, see e.g. Uliczka and Kondziella (2006); Gourlay et al. (2015a) for model-scale test results, and Gourlay and Klaka (2007); Gourlay (2008a) for full-scale test results, which showed that around half of the ships measured trimmed bow-down and half of them stern-down. In the present full-scale trials, from Fig. 11, it is shown that SEAMAX STAMFORD and CMA CGM WAGNER generally trim bow-down, while MOL PARAMOUNT trims stern-down. The maximum unfiltered dynamic trim are: 0.77m by the bow for SEAMAX STAMFORD; 1.17m by the stern for MOL PARAMOUNT; and 0.97m by the bow for CMA CGM WAGNER. These values are corresponding to 0.32%, 0.42% and 0.37% of their L_{pp} respectively.

Gourlay and Klaka (2007) showed that container ships full-scale tested have little dynamic trim in most cases. This is evidenced by comparing with the results of dynamic trim based on full-scale measurements for bulk carriers (Ha et al. 2016), e.g. an average dynamic trim for three bulk carriers at their speeds between 8 and 9 knots was 0.21m approximately, while that of the three container ships in the present trials is 0.04m, the average absolute value of the filtered data, at the same speed ranges. However, it must be borne in mind that container ships tend to travel faster than bulk

carriers. The maximum filtered results from the present trials are: 0.24m at the speed of 16knots for SEAMAX STAMFORD; 0.30m at the speed of 12knots for MOL PARAMOUNT; and 0.31m at the speed of 15knots for CMA CGM WAGNER.

Dynamic trim seems to be affected by turning manoeuvres as the SEAMAX STAMFORD and CMA CGM WAGNER cases have increases in dynamic stern-down trim when the ship's turning is made, i.e. near the G1 buoy in the Deep Water Channel, and around 2 km away from the G1 buoy of the Entrance Channel. This effect was witnessed in Hong Kong container ship trials (Gourlay 2008a). As previously explained, however, the measured dynamic trim in the vicinity of the G1 buoy in the Deep Water Channel was also affected by changes in both ship speeds and water depths.

Dynamic heel

In this paper, dynamic heel means the ship's total change in heel (positive to starboard), relative to the static floating position, that includes wave-induced roll (Gourlay 2008a). Results are also shown with a low-pass filter applied to remove the effect of wave-induced roll. Fig. 12 presents measured dynamic heel for the three transits.

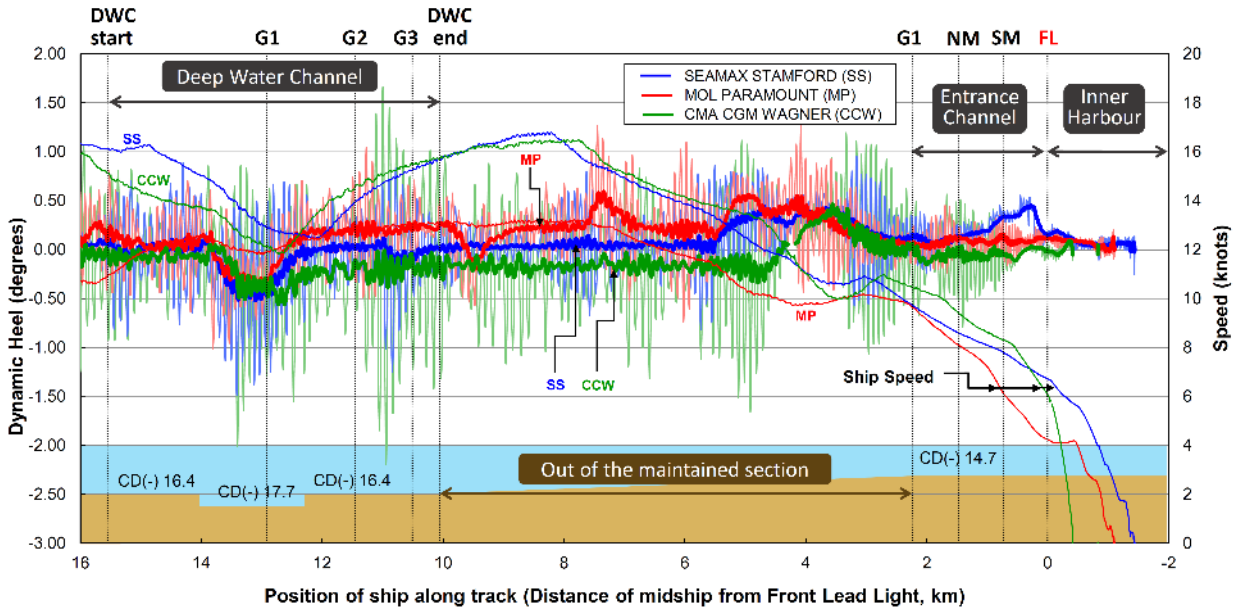

Fig. 12. Measured dynamic heel (positive to starboard) for the three ship transits (Note: Chart datum depth (not to scale) also shown)

Since container ships generally have small displacement to length ratio, high KG (vertical centre of gravity above keel) and low GM (metacentric height), large heel angles are experienced due to turning and wind (Gourlay and Klaka 2007). Furthermore, resonant rolling can occur for a ship when the wave encounter period is close to the ship's natural roll period (Ha et al. 2016). This means that dynamic heel may be the most important factor governing maximum sinkage for container ships, bringing the bilge corners closest to the seabed. For the container ships measured here, it can be confirmed that the influence of dynamic heel on the sinkage overwhelms that of dynamic trim by comparing the results of dynamic heel with the measured dynamic sinkage (see Fig. 10). SEAMAX STAMFORD and MOL PARAMOUNT have heel angles generally of the order 0.5° to 1.5°, the range of which causes one of the bilge corners to be closer to the seabed by: 0.16 - 0.49m for SEAMAX STAMFORD with the beam of 37.3m; and 0.17 - 0.52m for MOL PARAMOUNT with the beam of 40m. CMA CGM WAGNER travelled in the largest swell conditions (see Fig. 4) and hence had the largest heel oscillation angle of more than 2°. A 2° heel angle brings the bilge corner 0.7m closer to the seabed for CMA CGM WAGNER with the beam of 40m.

The effect of turning manoeuvres on dynamic heel is confirmed by the measurements. All transits have considerable heel angles to port when the ships turned to starboard around the G1 buoy in the Deep Water Channel, and another set of larger heel angles to starboard were also created when they made turns to port before entering the Entrance Channel.

Theoretical squat predictions

As the Deep Water Channel and the Entrance Channel have different channel depth, depths on the side of the channel and channel width, the relevant channel dimensions for predicting sinkage and trim need to be taken into account.

Information on suitable squat allowances for different types of channels and ships is addressed in the recent PIANC guidelines for harbour approach channels (Permanent International Association of Navigation Congresses (PIANC) 2014). Several semi-empirical methods (Hooft 1974; Huuska 1976; ICORELS 1980; Millward 1992) are based on the slender-body analysis of Tuck (1966) for

ships in shallow open water. According to that theory, the midship (midway of L_{PP}), bow and stern sinkage of a vessel should be given by

$$S_{mid} = C_{s\_mid} \frac{\nabla}{L_{PP}^{\ 2}} \frac{Fr_h^{\ 2}}{\sqrt{1 - Fr_h^{\ 2}}} \tag{1}$$

$$S_{bow} = C_{s\_bow} \frac{\nabla}{L_{PP}^{\ 2}} \frac{Fr_h^{\ 2}}{\sqrt{1 - Fr_h^{\ 2}}} \tag{2}$$

$$S_{stern} = C_{s\_stern} \frac{\nabla}{L_{PP}^{\ 2}} \frac{Fr_h^{\ 2}}{\sqrt{1 - Fr_h^{\ 2}}} \tag{3}$$

where Fr_h is the depth-based Froude number:

$$Fr_h = \frac{U}{\sqrt{gh}} \tag{4}$$

Here U is the ship speed, h is the water depth, and g is the gravitational acceleration. ∇ is the ship's displaced volume and L_{PP} is the ship's length between perpendiculars.

The nondimensional sinkage coefficients C_{s_mid}, C_{s_bow} and C_{s_stern} are predicted to be constant for each ship in open water, regardless of the ship speed or water depth. The sinkage coefficients should also be independent of scale. Gourlay (2013) and Ha and Gourlay (2017) showed how sinkage coefficients are affected by varying channel width, channel depth and side depth. An assessment was made to see whether a particular ship and channel configuration may be classed as open water, or whether a specific narrow-channel analysis is required. Based on the results in Ha and Gourlay (2017), with a Post-Panamax container ship (L_{PP} 260m), as in the ships analysed in the paper, the maximum sinkage coefficient for the Deep Water Channel is predicted within 1% of the open-water value, while that for the Entrance Channel is predicted to be within 10 - 15% of the open-water value. For theoretical squat predictions, therefore, the transits can be classed as open water condition and dredged channel condition for the Deep Water Channel and Entrance Channel respectively. Conceptual cross-sections of the channels are shown in Fig. 13.

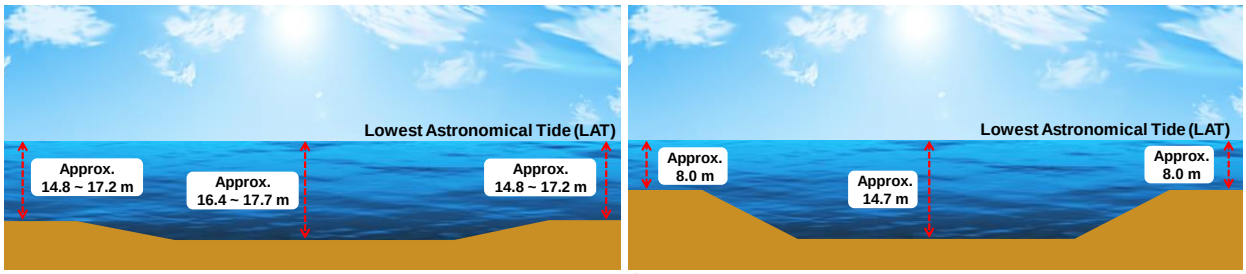

(a) (b)

Fig. 13. Conceptual cross section: (a) the Deep Water Channel; (b) the Entrance Channel (Note: These views are for illustration only (not to scale))

Theoretical method

The sinkage at midships (midway of L_{PP}) and the change in stern-down trim due to squat, are predicted using the slender-body theory of Tuck (1966) for open water and Beck et al. (1975) for dredged channels, generalized in Gourlay (2008c) and implemented in the computer code "SlenderFlow" (SlenderFlow 2017). The methods use linearized hull and free-surface boundary conditions. With Eqs. (1), (2) and (3) for the sinkage of a ship, the change in stern-down trim due to squat θ, can be written

$$\theta = C_\theta \frac{\nabla}{L_{PP}^{\ 3}} \frac{Fr_h^{\ 2}}{\sqrt{1 - Fr_h^{\ 2}}} \qquad (5)$$

where C_θ is the trim coefficient. For wide channels, the slender-body theory has been shown to give good results for container ships at model-scale (Gourlay et al. 2015a) and at full-scale (Gourlay 2008a).

Ship hull forms modelled

Without lines plans or exact hull offsets, published representative ship models that have similar characteristics to the practical hulls should be selected for the theoretical predictions. There are a number of publicly-available container ship hull forms which can be used, including:

- "Duisburg Test Case" ("DTC", 355m L_{PP}), designed by the University of Duisburg-Essen, Germany in 2012, representative of a 14,000 TEU Post-Panamax container ship (el Moctar et al. 2012)

- "KRISO Container Ship" ("KCS", 230m L_{PP}), designed by Korean Research Institute Ships and Ocean Engineering (KRISO) in 1997, representative of a 3,600 TEU Panamax container ship (Lee et al. 2003)
- "JUMBO" (320m L_{PP}), designed by SVA Potsdam, Germany in 1995, representative of a 5,500 TEU Post-Panamax container ship (Uliczka et al. 2004)
- "MEGA-JUMBO" (360m L_{PP}), designed by VWS Berlin, Germany in 2001, the design ship for the Jade Weser port in Germany, representative of a 12,000 TEU Post-Panamax container ship (Uliczka et al. 2004)
- "FHR Ship D" (291.13m L_{PP}), designed by Flanders Hydraulics Research and Ghent University, Belgium in 1996-2000, representative of a Post-Panamax container ship (Vantorre and Journée 2003; Gourlay et al. 2015b)
- "FHR Ship F" (190m L_{PP}), designed by Flanders Hydraulics Research and Ghent University, Belgium in 1996-2000, representative of a Panamax container ship (Vantorre and Journée 2003; Gourlay et al. 2015b)

Table 8. Details of the container ships measured and candidate ship hull forms

Cases	Ships & Hulls	L_{PP} (m)	Beam (m)	Draught (m)	C_B (-)	LCB (%)	LCF (%)
Container ships measured	SEAMAX STAMFORD	238.35	37.30	13.00 (at summer)	0.673	48.64	44.75
				10.83 (at actual)	0.634	49.42	46.86
	MOL PARAMOUNT	276.00	40.00	14.02 (at summer)	0.628	47.17	42.87
				11.39 (at actual)	0.574	48.21	45.67
	CMA CGM WAGNER	263.00	40.00	14.52 (at summer)	0.620	-	-
				10.75 (at actual)	0.548	-	-
Candidate ship hull forms	DTC	355.00	51.00	14.50	0.660	49.04	45.38
	KCS	230.00	32.20	10.80	0.650	48.52	44.33
	JUMBO	320.00	40.00	14.50	0.721	49.30	45.84
	MEGA-JUMBO	360.00	55.00	16.00	0.681	49.97	49.12
	FHR Ship D	291.13	40.25	15.00	0.604	47.05	44.54
	FHR Ship F	190.00	32.00	11.60	0.600	47.74	45.43

The principal details of these candidates and the three container ships measured are shown in Table 8. Here, block coefficient (C_B) are values at summer and actual draught for each container ship measured, and at design draught for the candidate ship hull forms. LCB and LCF are given as % of L_{PP} forward of the AP.

The KCS has been chosen for the SEAMAX STAMFORD transit, and the FHR Ship D for both the MOL PARAMOUNT and CMA CGM WAGNER transits. A minimum modification was a priority in selecting the reference hull for each transit. Changing ship hull shape has a significant effect on trim with a relatively small effect on sinkage (Uliczka and Kondziella 2006; Gourlay et al. 2015a; Ha and Gourlay 2017).

Modelling at reduced draught

Modification of the reference hull should be made to match the main hull parameters at the ship's actual transit conditions and, hence, at reduced draught. A general procedure for the modifications can be made as follows:

- A representative hull is chosen, with similar ship dimensions as well as dimensionless parameters such as C_B and LCB to each ship being modelled, e.g. the KCS and FHR Ship D
- The selected hulls are scaled to the same length (L_{PP}), beam and midships draught as the ships being modelled
- Parametric transformation is done by using MAXSURF Modeler to match desired hull parameters and hydrostatic properties

Based on the actual load and ballast conditions (see Table 2 and Table 8) as well as the above procedure, three ship models have been made from the supplied IGES files, e.g. a model ship using the KCS for SEAMAX STAMFORD and two different model ships using the FHR ship D for MOL PARAMOUNT and CMA CGM WAGNER respectively. Fig. 14 shows body plans of the KCS and FHR ship D with the bow, stern, profile, bottom and perspective views of the modelled ships.

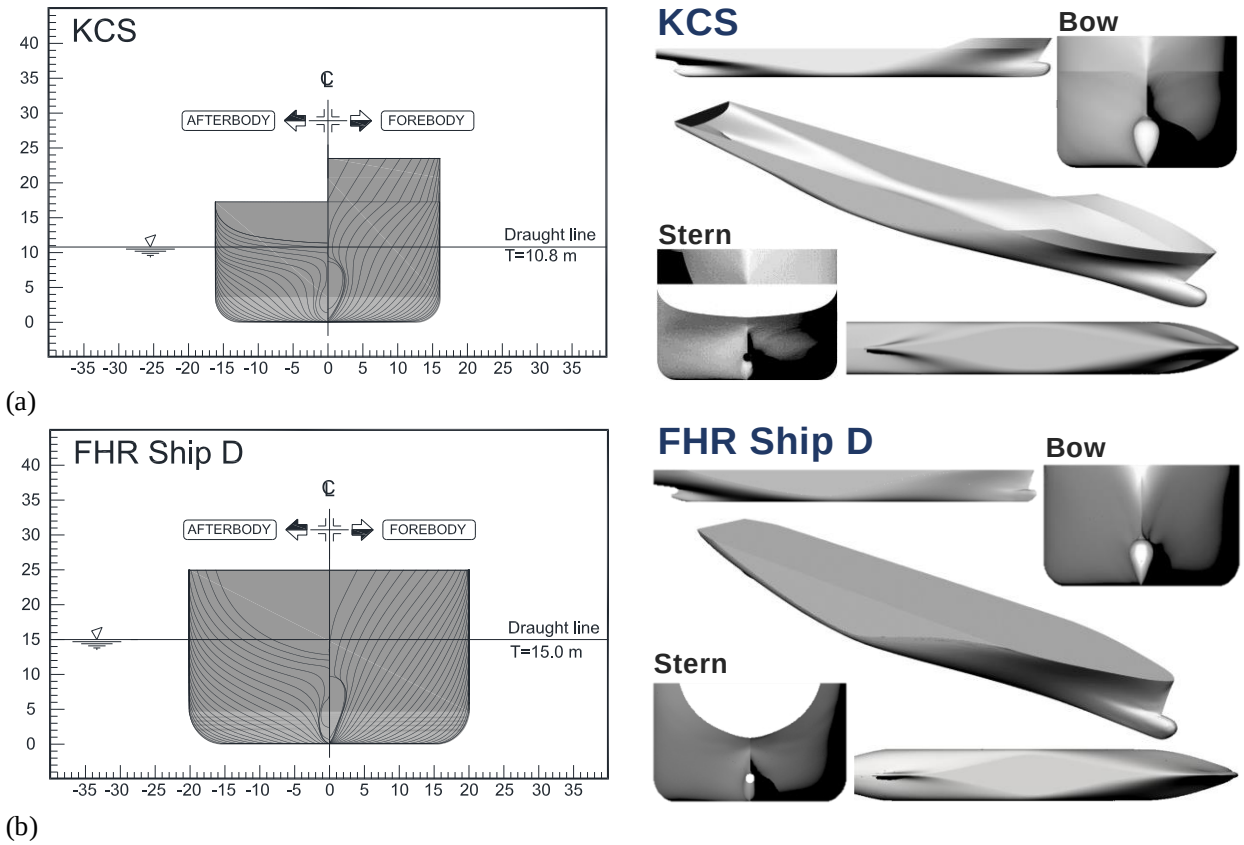

Fig. 14. Body plans and rendered views of the modelled ships: (a) KCS; (b) FHR Ship D

Results

Comparisons between measured and calculated sinkage at midships, together with ship speed and channel bathymetry, are shown in Fig. 15.

According to Gourlay et al. (2015a), the rectangular-canal slender-body theory (Tuck 1967) predicts the sinkage very close to the model test results for the wide-canal cases, in which channel effects are minimal, but under-predicts the sinkage in narrow canals. Note that no model tests approximating open-water dredged channels are available with which to compare. Here, in the predictions with the full-scale test results, it is shown that the measured midship sinkage agrees quite well with the predicted midship sinkage, especially, in the Deep Water Channel, classed as open water. However, the theory (Tuck 1966) is seen to slightly over-predict the sinkage for all the transits on the whole. The predicted midship sinkage, within the Deep Water Channel, are on average 9% larger than the measurements for SEAMAX STAMFORD; 7% for MOL PARAMOUNT; and 16% for CMA CGM WAGNER. This is the opposite of results in Gourlay

(2008a) which shows that the theoretical method (Tuck 1966) generally under-predicts the sinkage in Hong Kong. However, an exact comparison is not possible due to many uncertainties in applying the theory to the full-scale measurements, such as the complex bathymetry and the effect of the approximated hull geometry. These factors all could make application of the theory complicated.

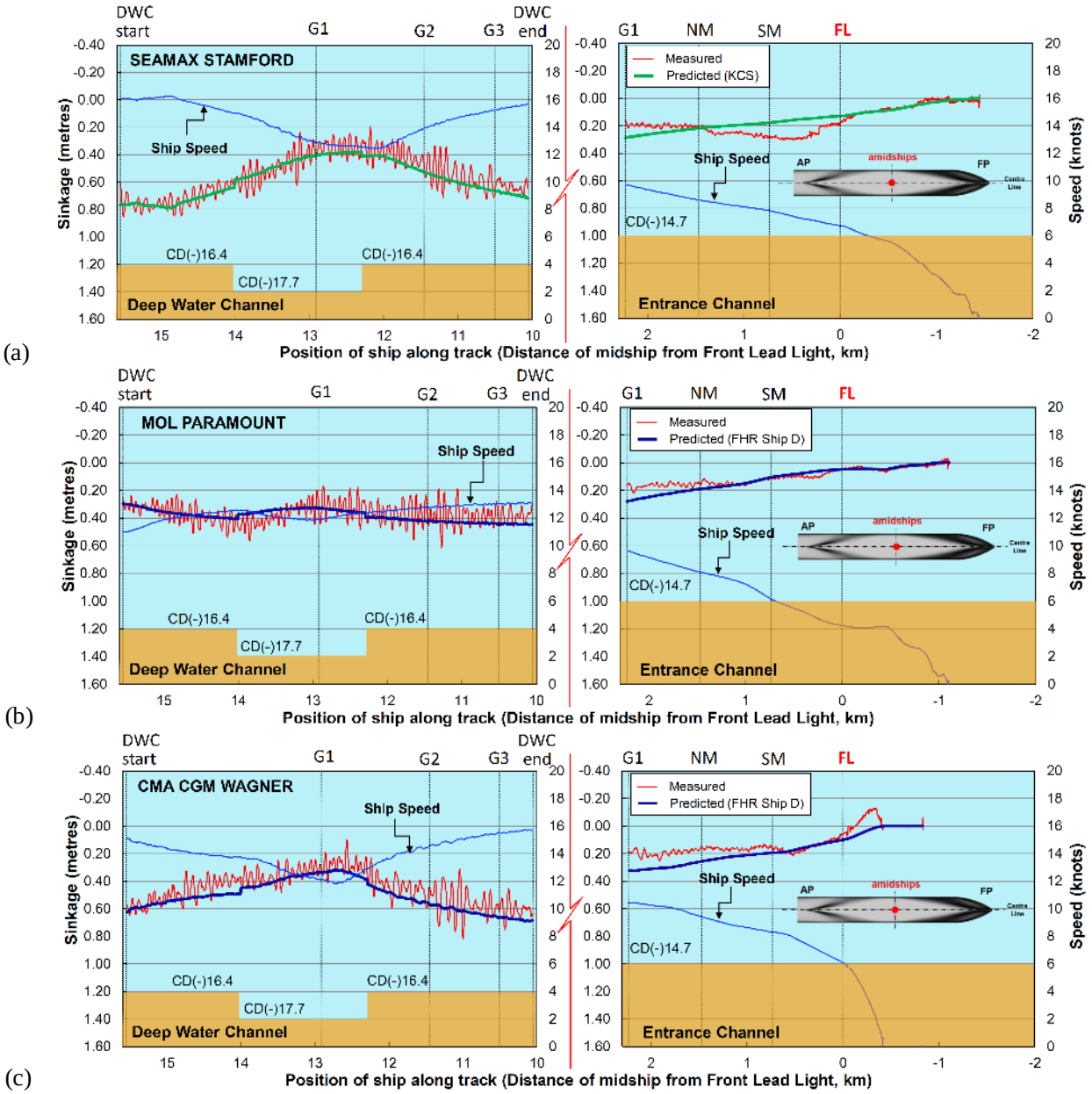

Fig. 15. Measured and calculated sinkage (positive downward) at midships: (a) SEAMAX STAMFORD; (b) MOL PARAMOUNT; (c) CMA CGM WAGNER (Note: Measured results are unfiltered and calculations do not include wave-induced motions; Chart datum depth (not to scale) also shown)

Dynamic trim is more difficult to predict than sinkage, as it is caused by the difference between large quantities: the downward force at the forward and aft shoulder; and the upward force at the bow and stern. Small changes in hull shape will change the balance between each of these. The effect of hull shape on dynamic trim is discussed in Gourlay et al. (2015a). Fig. 16 shows comparisons between measured and predicted dynamic trim. Dynamic trim is given here in degrees (°).

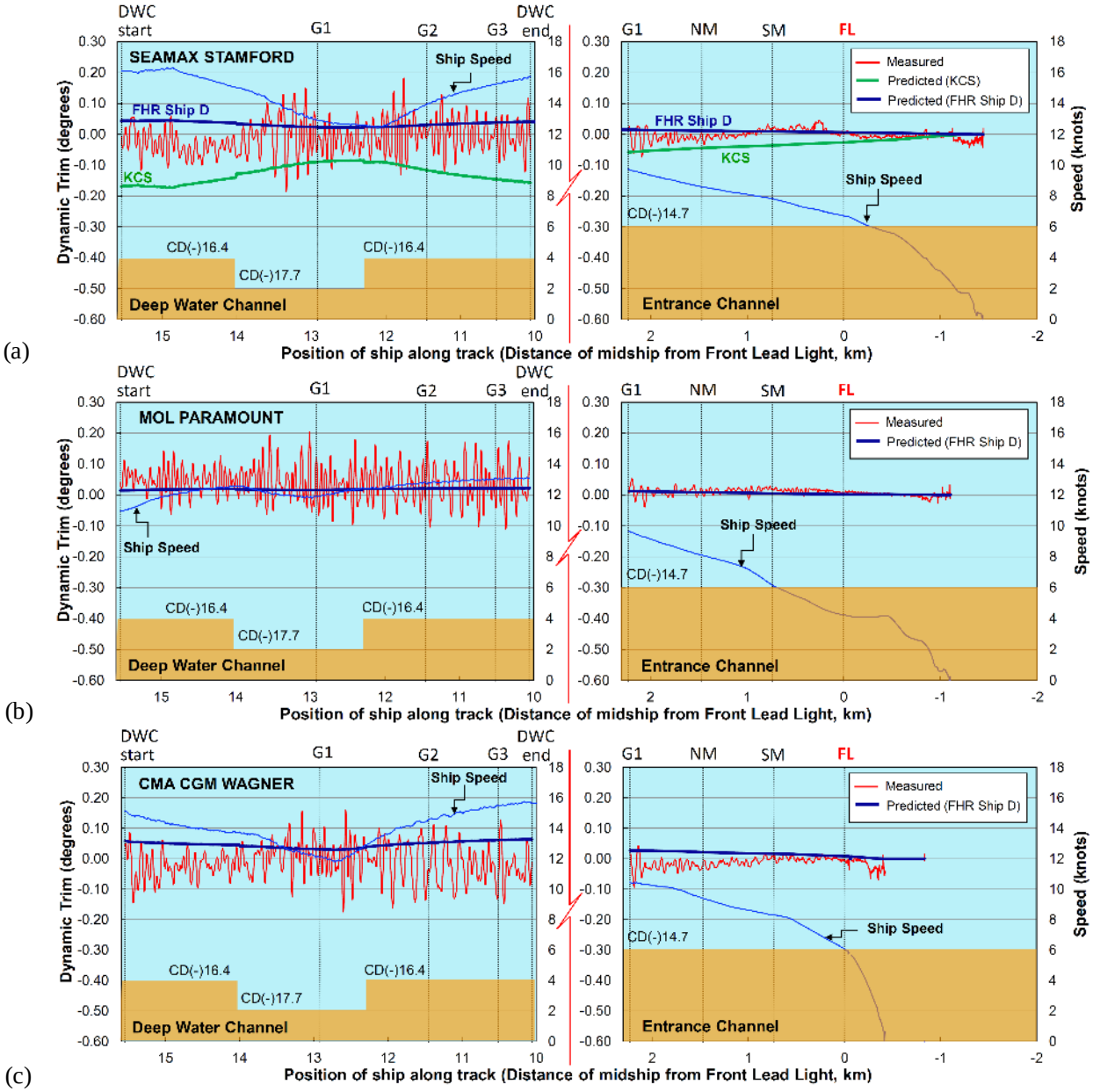

Fig. 16. Measured and calculated dynamic trim (positive stern-down): (a) SEAMAX STAMFORD; (b) MOL PARAMOUNT; (c) CMA CGM WAGNER (Note: Measured results are unfiltered and calculations do not include wave-induced motions; Chart datum depth (not to scale) also shown)

From Fig. 16, it is shown that the predicted dynamic trim is generally negative (bow-down) for SEAMAX STAMFORD using the KCS hull and positive (stern-down) for both MOL PARAMOUNT and CMA CGM WAGNER using the FHR Ship D hull.

In comparison with the measurements, the predicted dynamic trim for SEAMAX STAMFORD and MOL PARAMOUNT are more bow-down (or less stern-down) than the measured, whereas CMA CGM WAGNER shows a predicted dynamic trim that is slightly less bow-down (or more stern-down). With the fact that the modelled hull forms are approximate for the predictions, it is found that dynamic trim is reasonably well predicted by the theoretical method at full-scale.

Additionally, as shown in Fig. 16(a), two modelled ship hulls, i.e. the KCS and FHR Ship D, have been applied to the SEAMAX STAMFORD case in order to see the effect of hull geometry on dynamic trim. The two modelled ships have been modified to match SEAMAX STAMFORD's hull parameters at its actual transit conditions, and hence they should have similar characteristics of the hull such as block coefficient (C_B) and LCB. Nonetheless, they show conflicting results of dynamic trim with the KCS having a negative trim (bow-down) and the FHR Ship D having a positive trim (stern-down). This epitomizes how sensitive dynamic trim is to the hull shape and hence the importance of acquiring the ship's full lines plans or exact hull offsets for predictions. Note that less modification was made for the KCS due to its original resemblance to the SEAMAX STAMFORD hull.

Conclusions

High-quality data for vertical ship motions in port approach channels have been obtained from the set of recent full-scale trials of container ships using high-accuracy GNSS receivers and a fixed reference station. Dynamic sinkage, trim and heel of three container ship transits have been analysed in more detail from a total of 16 ship measurements in the Port of Fremantle. These trial results have been applied to the validation of numerical ship motion modelling at full-scale. In future work, the measured results will be used for validating wave-induced motions software.

Estimated errors involved in calculating dynamic sinkage have been analysed including the effects of the GNSS receivers' error, geoid undulation error, static reading error and tide-related errors.

The total RMS error in downward sinkage of each point on the hull was estimated to be around 0.040m in the Deep Water Channel, and 0.039m in the Entrance Channel and Inner Harbour.

For the three container ships analysed here (SEAMAX STAMFORD; MOL PARAMOUNT; CMA CGM WAGNER), two transits (MOL PARAMOUNT; CMA CGM WAGNER) have maximum sinkage at the starboard bilge corner, and another case (SEAMAX STAMFORD) at the bow, which range between: 0.33% and 0.48% of L_{PP}; 7.96% and 11.81% of the static draught. Two (SEAMAX STAMFORD; CMA CGM WAGNER) out of the three transits showed that the stern could have maximum dynamic draught due to its already close proximity to the seabed. Dynamic draught increase of the point on the ship having the maximum dynamic draught ranged from 7.62% to 7.96% of the static draught. Elevations of the ship's keel relative to Chart Datum have also been calculated for practical UKC (Under-Keel Clearance) management.

Regarding dynamic trim, no clear trend was found in the present full-scale measurements, showing two transits (SEAMAX STAMFORD; CMA CGM WAGNER) trim bow-down and the other (MOL PARAMOUNT) trims stern-down. The overall dynamic trim of the container ships was much less than that of bulk carriers measured in full-scale trials.

The effect of dynamic heel on the sinkage generally overwhelmed that of dynamic trim for the three container ships. The effect of turning manoeuvres on dynamic heel was confirmed by the measurements. A maximum heel angle of more than 2°, and heel angles generally of the order 0.5° to 1.5°, were measured for the three Post-Panamax container ships.

A theoretical method using slender-body shallow-water theory has been applied to predict the measured sinkage and trim of the transits. The slender-body theory is able to predict squat (steady sinkage and trim) with reasonable accuracy for container ships at full-scale in open dredged channels.

Appendix. Elevations of the ship's keel relative to Chart Datum

In this appendix, elevations of the ship's keel relative to chart datum for (a) SEAMAX STAMFORD, (b) MOL PARAMOUNT and (c) CMA CGM WAGNER are plotted, as shown in Fig.17.

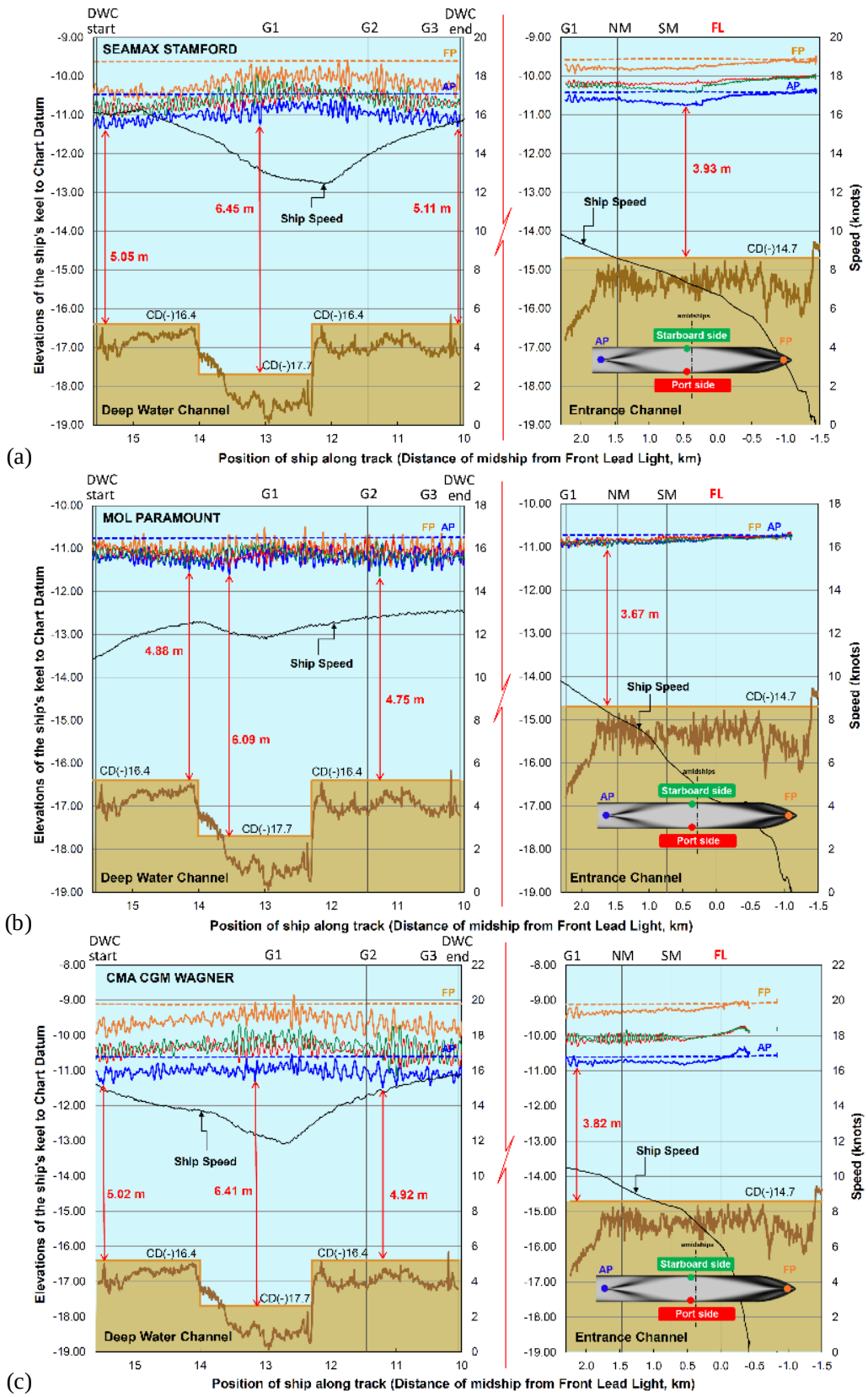

Fig. 17. Elevations of the ship's keel relative to chart datum: (a) SEAMAX STAMFORD; (b) MOL PARAMOUNT; (c) CMA CGM WAGNER

Dashed lines near the top of the figures are elevations of the FP (orange) and AP (blue) including changes in tide only (see Table 7), i.e. their static position, not including squat and wave-induced motions. This shows how much of the vertical movement is due to tide changes (Ha et al. 2016). A flat seabed line is based on the charted depth on AUS 112, and a fluctuating seabed line is the actual survey line provided by Fremantle Ports.

Acknowledgements

The authors wish to thank all of the marine pilots and staff at Fremantle Ports for their assistance, support and enthusiasm in conducting the trials. The authors would also like to acknowledge the following organizations for their contributions to this research: Seamax Shipping, Tokei Kaiun and CMA CGM, who provided access to and hull information for SEAMAX STAMFORD, MOL PARAMOUNT and CMA CGM WAGNER respectively; Flanders Hydraulics Research and Ghent University, who provided hull data for Ship D; and OMC International, who provided surveyed depth data for the channels. The contribution of an Australian Government Research Training Program Scholarship in supporting this research is acknowledged by the authors.

References

AutoCAD [Computer software]. Autodesk, San Rafael, California.

Beck, R.F., Newman, J.N., and Tuck, E.O. (1975). "Hydrodynamic forces on ships in dredged channels." *Journal of Ship Research*, 19(3), 166-171.

Brown, N.J., Featherstone, W.E., Hu, G., and Johnston, G.M. (2011). "AUSGeoid09: a more direct and more accurate model for converting ellipsoidal heights to AHD heights." *Journal of Spatial Science*, 56(1), 27-37.

Dand, I.W., and Ferguson, A.M. (1973). "The squat of full ships in shallow water." *Transactions of the Royal Institution Naval Architects (RINA)*, 115, 237-255.

Deng, G.B., Guilmineau, E., Leroyer, A., Queutey, P., Visonneau, M., and Wackers, J. (2014). "Simulation of container ship in shallow water at model scale and full scale." *Proc., 3rd Chinese National CFD Symposium on Ship and Offshore Engineering*, Dalian, China.

el Moctar, O., Shigunov, V., and Zorn, T. (2012). "Duisburg Test Case: Post-panamax container ship for benchmarking." *Ship Technology Research*, 59(3), 50-64.

Featherstone, W.E., Kirby, J.F., Hirt, C., Filmer, M.S., Claessens, S.J., Brown, N.J., Hu, G., and Johnston G.M. (2011). "The AUSGeoid09 model of the Australian Height Datum." *Journal of Geodesy*, 85(3), 133-150.

Feng, Y., and O'Mahony, S. (1999). "Measuring ship squat, trim, and under-keel clearance using on-the-fly kinematic GPS vertical solutions." *Journal of the Institute of Navigation*, 46(2), 109-117.

Ferguson, A.M., and McGregor, R.C. (1986). "On the squatting of ships in shallow and restricted water." *Proc., 20th International Conference on Coastal Engineering*, Taipei, Taiwan, 2772-2786.

Fremantle Ports. (2011). *Port Information Guide*, Fremantle Ports, Fremantle, Western Australia, <http://www.fremantleports.com.au/sitecollectiondocuments/port%20information%20guide.pdf>.

Gourlay, T.P. (2006). "Flow beneath a ship at small under keel clearance." *Journal of Ship Research*, 50(3), 250-258.

Gourlay, T.P. (2007). "Ship underkeel clearance in waves." *Proc., Coasts and Ports 2007 Conference*, Melbourne, Australia.

Gourlay, T.P. (2008a). "Dynamic draught of container ships in shallow water." *International Journal of Maritime Engineering*, 150(4), 43-56.

Gourlay, T.P. (2008b). "Validation of KeelClear software in Torres Strait." *CMST Report 2008-05*, Centre for Marine Science and Technology, Curtin University, Bentley, Western Australia, <http://cmst.curtin.edu.au/wp-content/uploads/sites/4/2016/08/CMST-ARP-KeelClear-validation-in-Torres-Strait.pdf>.

Gourlay, T.P. (2008c). "Slender-body methods for predicting ship squat." *Ocean Engineering*, 35(2), 191-200.

Gourlay, T.P. (2013). "Ship squat in non-uniform water depth." *Proc., Coasts and Ports 2013 Conference*, Manly, Australia.

Gourlay, T.P., and Klaka, K. (2007). "Full-scale measurements of containership sinkage, trim and roll." *Australian Naval Architect*, 11(2), 30-36.

Gourlay, T.P., Ha, J.H., Mucha, P., and Uliczka, K. (2015a). "Sinkage and trim of modern container ships in shallow water." *Proc., Coasts and Ports 2015 Conference*, Auckland, New Zealand.

Gourlay, T.P., Von Graefe, A., Shigunov, V., and Lataire, E. (2015b). "Comparison of AQWA, GL RANKINE, MOSES, OCTOPUS, PDSTRIP and WAMIT with model test results for cargo ship wave-induced motions in shallow water." *Proc., ASME 34th International Conference on Ocean, Offshore and Arctic Engineering*, OMAE 2015, St. John's, Newfoundland, Canada.

Gourlay, T.P., Lataire, E., and Delefortrie, G. (2016). "Application of potential flow theory to ship squat in different canal widths." *Proc., 4th International Conference on Ship Manoeuvring in Shallow and Confined Water*, MASHCON 2016, Hamburg, Germany, 146-155.

Graff, W., Kracht, A., and Weinblum, G. (1964). "Some extensions of D. W. Taylor's standard series." *Transactions of the Society of Naval Architects and Marine Engineers*, 72, 374-401.

Ha, J.H., and Gourlay, T.P. (2016). "Ship motion measurements for ship under-keel clearance in the Port of Fremantle." *CMST Report 2016-07,* Centre for Marine Science and Technology, Curtin University, Bentley, Western Australia, <http://cmst.curtin.edu.au/wp-content/uploads/sites/4/2016/09/ Ha-2016-Ship-motion-measurements-for-ship-under-keel-clearance-in-the-Port-of-Fremantle.pdf>.

Ha, J.H., and Gourlay, T.P. (2017). "Bow and stern sinkage coefficients for cargo ships in shallow open water." The third-place winner of the 2017 PIANC De Paepe-Willems Award, in press.

Ha, J.H., Gourlay, T.P., and Nadarajah, N. (2016). "Measured ship motions in Port of Geraldton approach channel." *Proc., 4th International Conference on Ship Manoeuvring in Shallow and Confined Water*, MASHCON 2016, Hamburg, Germany, 236-250.

Härting, A., and Reinking, J. (2002). "SHIPS: A new method for efficient full-scale ship squat determination." *Proc., 30th PIANC-AIPCN Congress*, Sydney, Australia, 1805-1813.

Härting, A., Laupichler, A., and Reinking, J. (2009). "Considerations on the squat of unevenly trimmed ships." *Ocean Engineering*, 36(2), 193-201.

Hatch, T. (1999). "Experience measuring full scale squat of full form vessels at Australian ports." *Proc., Coasts and Ports 1999 Conference,* Perth, Australia.

Hooft, J.P. (1974). "The behaviour of a ship in head waves at restricted water depth." *International Shipbuilding Progress*, 21(244), 367-378.

Huuska, O. (1976). "On the evaluation of underkeel clearances in Finnish waterways." *Ship Hydrodynamics Laboratory Report No. 9*, Helsinki University of Technology, Otaniemi, Finland.

ICORELS (International Commission for the Reception of Large Ships). (1980). "Report of Working Group IV." *supplement to PIANC Bulletin No. 35*.

JAVAD. (2012). *JAVAD TRIUMPH-1 Integrated GNSS Receiver Operator's Manual Version 2.0*, JAVAD GNSS®, California, USA.

JAVAD. (2015). *JAVAD TRIUMPH-2 Datasheet*, JAVAD GNSS®, California, USA.

Lee, S.J., Koh, M.S., and Lee, C.M. (2003). "PIV velocity field measurements of flow around a KRISO 3600TEU container ship model." *Journal of Marine Science and Technology*, 8(2), 76-87.

MATLAB [Computer software]. The MathWorks, Natick, Massachusetts.

MAXSURF Modeller [Computer software]. Bentley Systems, Exton, Pennsylvania.

Microsoft Excel [Computer software]. Microsoft, Redmond, Washington.

Millward, A. (1992). "A comparison of the theoretical and empirical prediction of squat in shallow water." *International Shipbuilding Progress*, 39(417), 69-78.

Mucha, P., el Moctar, O., and Böttner, C.U. (2014). "Technical note: PreSquat - Workshop on numerical prediction of ship squat in restricted waters." *Ship Technology Research*, 61(3), 162-165.

NGA (National Geospatial-intelligence Agency). (2014). "North, West, and South Coasts of Australia." *PUB. 175 Sailing Directions (Enroute), Twelfth Edition*.

PIANC (Permanent International Association of Navigation Congresses). (2014). "Harbour Approach Channels Design Guidelines." *PIANC Report No. 121*.

SlenderFlow [Computer software]. Perth Hydro, Perth, Western Australia.

"SlenderFlow." (2017). *Perth Hydro*, <http://www.slenderflow.com> (Jan.11, 2017).

Trimble Business Centre [Computer software]. Trimble, Sunnyvale, California.

Tuck, E.O. (1966). "Shallow water flows past slender bodies." *Journal of Fluid Mechanics*, 26, 81-95.

Tuck, E.O. (1967). "Sinkage and trim in shallow water of finite width." *Schiffstechnik*, 14, 92-94.

Uliczka, K., and Kondziella, B. (2006). "Dynamic response of very large container ships in extremely shallow water." *Proc., 31st PIANC Congress*, Estoril, Portugal.

Uliczka, K., Kondziella, B., and Flügge, G. (2004). "Dynamisches fahrverhalten sehr großer containerschiffe in seitlich begrenztem extremen Flachwasser [Dynamic behaviour of very

large container ships in extremely confined and shallow water].” *HANSA*, 141, Jahrgang, Nr. 1 (in German).

U.S. NRL (U.S. Naval Research Laboratory). (n.d.). “Tides and Currents in Fremantle.” <https://www.nrlmry.navy.mil/port_studies/thh-nc/australi/fremantl/text/sect6.htm> (May.25, 2017).

Vantorre, M., and Journée, J.M.J. (2003). “Validation of the strip theory code SEAWAY by model tests in very shallow water.” *Proc., Numerical Modelling Colloquium (DUT-SHL Report Nr. 1373-E)*, Flanders Hydraulics Research, Antwerp, Belgium.

Verstraete, J.M. (2001). *Sea-level changes and their effects: Low frequency sea level variability in the western tropical pacific 1992-1998*, World Scientific Publishing, Singapore.